

## Li-insertion/extraction Properties of Si Thick-film Anodes in Ionic Liquid Electrolytes Based on Bis(fluorosulfonyl)amide and Bis(trifluoromethanesulfonyl)amide Anions

Hiroyuki Usui, Toshikazu Masuda, and Hiroki Sakaguchi\*

Department of Chemistry and Biotechnology, Graduate School of Engineering, Tottori University,  
4-101 Minami, Koyama-cho, Tottori 680-8552

(Received February 7, 2012; CL-120099; E-mail: sakaguch@chem.tottori-u.ac.jp)

Charge–discharge cycling performances of Si thick-film electrodes as Li-ion battery anodes were investigated in several ionic liquids based on bis(fluorosulfonyl)amide (FSA) and bis(trifluoromethanesulfonyl)amide (TFSA) anions. The Si electrodes in FSA-based electrolytes exhibited much better performance than those in TFSA-based electrolytes. An easier desolvation of Li from anions on the electrode surface is probably promoted in FSA-based electrolytes, which enables efficient electrode reactions of Li-insertion/extraction and improvement of cycling performances.

Ionic liquid electrolytes are highly anticipated to be applied to graphite anodes<sup>1,2</sup> and Si-based anodes<sup>3</sup> in Li-ion batteries. No remarkable study has been, however, performed for ionic liquid electrolytes applied for pure Si anode. Aurbach et al. have reported that a sputtered Si film anode with 100 nm in thickness exhibited good cycling performance in an ionic liquid electrolyte.<sup>3</sup> By contrast, the authors believe that the performance should be evaluated for a film thick enough for practical use, and have recently investigated anode properties of thick-film electrodes prepared by a gas-deposition (GD) method.<sup>4,5</sup> The most notable point is that this method does not require any binder and conductive additive to prepare thick-film electrodes. It is therefore possible to clarify an original anode property of pure Si electrode. In this study, we evaluated charge–discharge cycling performances of Si thick-film electrodes as Li-ion battery anode in several ionic liquid electrolytes, and investigated the effect of their molecular structures on their anode performances.

Silicon thick-film electrodes were prepared on Cu foil substrates by GD of a commercial Si powder (purity: 99.9%) using Ar carrier gas. Further detailed conditions have been described in our previous reports.<sup>4,5</sup> The thickness of obtained Si film was not uniform and the typical thickness was 3 μm. As solvents of electrolytes, six kinds of ionic liquids were used in this study. These structural formulas and physical properties<sup>6</sup> are summarized in Figure 1 and Table 1, respectively. The conductivity was measured. The cations are *N*-methyl-*N*-propylpiperidinium (PP13), *N*-methyl-*N*-propylpyrrolidinium (Py13), and 1-ethyl-3-methylimidazolium (EMI). The anions are bis(fluorosulfonyl)amide (FSA) and bis(trifluoromethanesulfonyl)amide (TFSA). PP13–TFSA was developed by Matsumoto et al.<sup>7</sup> Electrolytes were prepared by dissolving a salt of Li–TFSA in these ionic liquids with a concentration of 1.0 M. For comparison, we used an electrolyte of 1.0 M LiClO<sub>4</sub>-dissolved propylene carbonate (PC, C<sub>4</sub>H<sub>6</sub>O<sub>3</sub>) as a conventional organic electrolyte. Coin-type 2032 size cells were assembled using working electrodes of Si films, counter electrodes of Li sheets, and polypropylene separators.<sup>5</sup> Before the cell assembly, the separators were immersed in the electrolytes for 30 min in vacuum. Constant current charge–discharge tests were carried out at 303 K under 0.42 A g<sup>-1</sup> (0.1 C). An electrochemical impedance spectroscopic (EIS) analysis was performed at 0.005 V vs. Li/Li<sup>+</sup> in the range of 100 kHz–10 mHz. Nyquist plots were

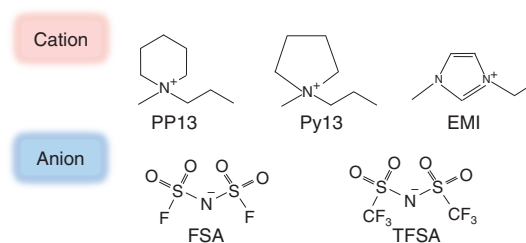


**Figure 1.** Structural formulas of cations and anions in ionic liquid electrolytes. Cations are *N*-methyl-*N*-propylpiperidinium (PP13), *N*-methyl-*N*-propylpyrrolidinium (Py13), and 1-ethyl-3-methylimidazolium (EMI). Anions are bis(fluorosulfonyl)amide (FSA) and bis(trifluoromethanesulfonyl)amide (TFSA).

**Table 1.** Summary for anode performances of Si thick-film electrodes in several ionic liquid electrolytes<sup>a</sup>

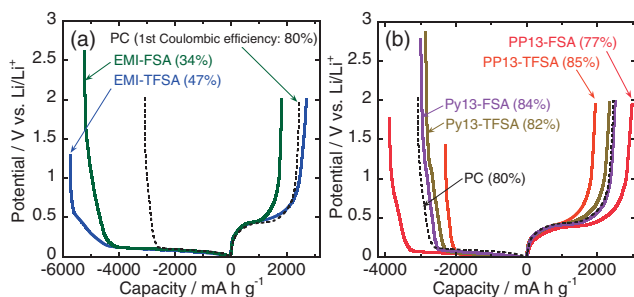
Solvent		Viscosity <sup>6</sup> /mPa s	Conductivity /mS cm <sup>-1</sup>	Discharge capacity /mA h g <sup>-1</sup>		Initial Coulombic efficiency /%
Cation	Anion			1st	150th	
PP13	FSA	95	4.0	2980	1420	77
	TFSA	151	1.7	1940	810	85
Py13	FSA	40	8.3	2500	1330	84
	TFSA	61	4.0	2360	820	82
EMI	FSA	18	17.7	1820	980	34
	TFSA	33	9.1	2700	190	47
PC		2.3	5.3	2460	68	80

<sup>a</sup>This table also shows the viscosity<sup>6</sup> and conductivity of these ionic liquids without Li salt. The conductivity of PC was measured with Li salt.

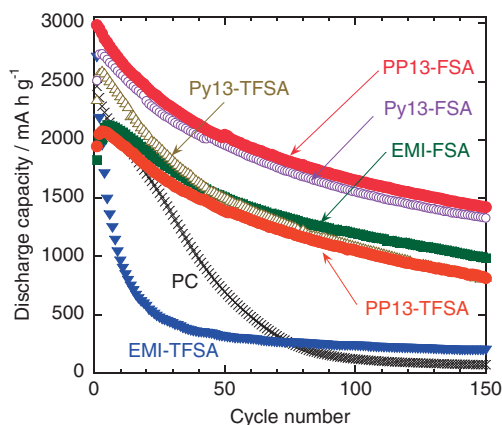
analyzed by using Randles circuit<sup>8</sup> containing surface film resistance  $R_{sf}$  and charge transfer resistance  $R_{ct}$  (Figure S2<sup>12</sup>).

Figure 2 shows charge–discharge curves at the first cycles of the Si thick-film electrodes in various ionic liquid electrolytes. In every case, potential plateaus appeared at 0.1 and 0.4 V vs. Li/Li<sup>+</sup> in charge (lithiation) and discharge (delithiation) processes, which originated from alloying/dealloying reactions of Li–Si. In case of EMI–TFSA electrolyte shown in Figure 2a, we can recognize a low Coulombic efficiency of 47% and a potential shoulder at around 0.5 V on account of a cathodic decomposition of the cation. The decomposition occurs by an initial attack on an acidic proton attached to the ring carbon between two nitrogens, which leads to a successive alkylation of the ring.<sup>9</sup> In contrast, relatively high efficiencies of around 80% were obtained in the electrolytes based on PP13 and Py13 cations as shown in Figure 2b. In particular, the largest discharge capacity of 2980 mA h g<sup>-1</sup> was attained at the first cycle of discharge in PP13–FSA.

Figure 3 depicts cycling performances of these Si anodes. Generally, Si anodes show a significant capacity decay in conven-



**Figure 2.** Initial charge–discharge curves of Si thick-film anodes in various ionic liquid electrolytes: (a) EMI–TFSA and EMI–FSA, (b) PP13–TFSA, PP13–FSA, Py13–TFSA, and Py13–FSA.



**Figure 3.** Cycling performances of Si thick-film electrodes in various ionic liquid electrolytes.

tional electrolytes. The origin is pulverization of Si induced by accumulated stress due to its volume changes during Li-insertion/extraction. This is more pronounced for a thick-film anode because the volume cannot easily change because of its large film-thickness. In this study, we observed the capacity decay in PC. In the electrolyte of EMI–TFSA, the capacity was more rapidly decreased to  $300 \text{ mA h g}^{-1}$  by the 50th cycle, resulting in a very poor cyclability. In contrast, the electrode in EMI–FSA exhibited a remarkably improved performance and the capacity of  $980 \text{ mA h g}^{-1}$  even at the 150th cycle. High efficiencies ( $>97\%$ ) were maintained in EMI–FSA after the 15th cycle though the initial efficiency was very low. On the other hand, in EMI–TFSA, the efficiency was less than  $81\%$  at the 15th cycle. We suggested that the cathodic decomposition of EMI was relatively suppressed after several cycles by changing anion from TFSA to FSA, which was previously reported for a graphite anode by Ishikawa et al.<sup>2</sup>

The TFSA-based electrolytes with Py13 and PP13 cations exhibited performances as good as EMI–FSA. In the initial 40 cycles, Py13–TFSA is superior to PP13–TFSA in terms of the capacity. This is possibly related to its higher conductivity. When TFSA anions of the two electrolytes were changed to FSA anions, the anodes demonstrated further advanced performances. Among them, the most excellent cyclability was achieved in PP13–FSA: the discharge capacity of  $1420 \text{ mA h g}^{-1}$  was maintained even at 150th cycle.

The mechanism of the improved performances by FSA anions is discussed in the light of Li-ion transfer at the interface between electrolytes and electrodes. Although the fitting analysis of EIS

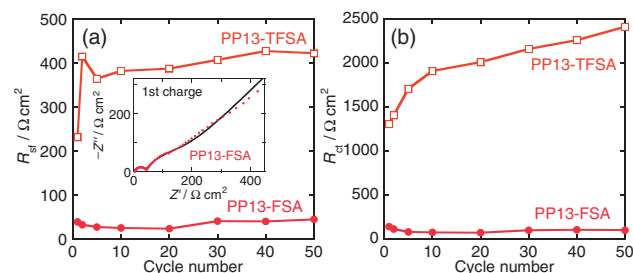


**Figure 4.** Variation in (a) surface film resistance ( $R_{sf}$ ) and (b) charge transfer resistance ( $R_{ct}$ ) for Si thick-film electrodes charged at potential of  $0.005 \text{ V vs. Li/Li}^+$  in ionic liquid electrolytes of PP13–TFSA and PP13–FSA. Inset of Figure 4a shows Nyquist plots for PP13–FSA at the first cycle and the fitting result.

is difficult, we here interpreted a part of Nyquist plots as a combination of two semicircles indicating  $R_{sf}$  and  $R_{ct}$ . Figure 4 compares  $R_{sf}$  and  $R_{ct}$  obtained by EIS analysis for the Si electrodes in PP13–FSA and PP13–TFSA. The  $R_{sf}$  and  $R_{ct}$  in PP13–TFSA were about ten times and twenty times larger than those in PP13–FSA, respectively. The much lower resistances clearly indicate that Li ions easily pass across a solid electrolyte interface layer or an electric double layer (Figure S3<sup>12</sup>), and that Li ions require less activation energy for desolvation from FSA. A conformation structure has been studied for Li ions solvated by TFSA and FSA.<sup>10,11</sup> The positive charges on sulfur atoms of FSA are substantially larger than those of TFSA, resulting in its smaller polarizability and weaker electrostatic interaction between Li and FSA.<sup>11</sup> The stabilization energy of Li–FSA cluster ( $-134.3 \text{ kcal mol}^{-1}$ ) is higher than that of Li–TFSA cluster ( $-137.2 \text{ kcal mol}^{-1}$ ),<sup>11</sup> supporting our consideration. Because of less interaction between Li ions and FSA, Li ions can be easily desolvated and can smoothly transfer, which is a possible reason for the suppressed decomposition of EMI by FSA anions. We therefore conclude that the easier desolvation of Li at the interface is probably promoted in the FSA-based electrolytes, which enables efficient electrode reactions of Li-insertion/extraction and improvement of cycling performances.

This work was partially supported by a grant from the Li-EAD Project from NEDO of Japan, and by Grant-in-Aid for Scientific Research of MEXT, Japan.

#### References and Notes

- H. Zheng, K. Jiang, T. Abe, Z. Ogumi, *Carbon* **2006**, *44*, 203.
- M. Ishikawa, T. Sugimoto, M. Kikuta, E. Ishiko, M. Kono, *J. Power Sources* **2006**, *162*, 658.
- V. Baranchugov, E. Markevich, E. Pollak, G. Salitra, D. Aurbach, *Electrochem. Commun.* **2007**, *9*, 796.
- a) H. Sakaguchi, T. Toda, Y. Nagao, T. Esaka, *Electrochem. Solid-State Lett.* **2007**, *10*, J146. b) H. Usui, H. Nishinami, T. Iida, H. Sakaguchi, *Electrochemistry* **2010**, *78*, 329. c) H. Usui, M. Shibata, K. Nakai, H. Sakaguchi, *J. Power Sources* **2011**, *196*, 2143.
- H. Usui, Y. Yamamoto, K. Yoshiyama, T. Itoh, H. Sakaguchi, *J. Power Sources* **2011**, *196*, 3911.
- H. Matsumoto, H. Sakaebe, K. Tatsumi, M. Kikuta, E. Ishiko, M. Kono, *J. Power Sources* **2006**, *160*, 1308.
- H. Sakaebe, H. Matsumoto, *Electrochem. Commun.* **2003**, *5*, 594.
- M. Egashira, A. Kanetomo, N. Yoshimoto, M. Morita, *J. Power Sources* **2011**, *196*, 6419.
- M. C. Buzzeo, R. G. Evans, R. G. Compton, *ChemPhysChem* **2004**, *5*, 1106.
- Y. Umabayashi, T. Mitsugi, S. Fukuda, T. Fujimori, K. Fujii, R. Kanzaki, M. Takeuchi, S.-I. Ishiguro, *J. Phys. Chem. B* **2007**, *111*, 13028.
- S. Tsuzuki, K. Hayamizu, S. Seki, *J. Phys. Chem. B* **2010**, *114*, 16329.
- Supporting Information is available electronically on the CSJ-Journal Web site, <http://www.csj.jp/journals/chem-lett/index.html>.